# On Generalized Borgen Plots.
# II: The line-moving algorithm and its numerical implementation.

Annekathrin Jürß[a], Mathias Sawall[a], Klaus Neymeyr[a,b]

[a]*Universität Rostock, Institut für Mathematik, Ulmenstraße 69, 18057 Rostock, Germany.*
[b]*Leibniz-Institut für Katalyse e.V. an der Universität Rostock, Albert-Einstein-Straße 29a, 18059 Rostock, Germany.*

## Abstract

Borgen plots are geometric constructions which represent the set of all nonnegative factorizations of spectral data matrices for three-component systems. The classical construction by Borgen and Kowalski (Anal. Chim. Acta 174, 1-26 (1985)), is limited to nonnegative data and results in nonnegative factorizations.

The new approach of generalized Borgen plots allows factors with small negative entries. This makes it possible to construct Borgen plots for perturbed or noisy spectral data and stabilizes the computation. In the first part of this paper the mathematical theory of generalized Borgen plots has been introduced. This second part presents the line-moving algorithm for the construction of generalized Borgen plots. The algorithm is justified and the implementation in the *FACPACK* software is validated.

*Key words:* factor analysis, Borgen plot, area of feasible solutions, tangent algorithm, line-moving algorithm.

## 1. Introduction

The systematic analysis of the non-uniqueness of pure component factorizations by multivariate curve resolution (MCR) methods is a challenging research area. Many results on the so-called rotational ambiguity and the area of feasible solutions have been gained in recent years. Historically, the starting points of such investigations are the Lawton-Sylvestre plots for two-component systems [8] and the Borgen plots for three-component systems [3, 10]. These plots are low-dimensional representations of the sets of feasible nonnegative pure component factorizations for spectral data matrices with their underlying bilinear structure of the Lambert-Beer law.

The pivotal point of these analyses are factorizations $D = CA$ of $k \times n$ spectroscopic data matrices $D$ with nonnegative factors $C$ and $A$. The rows of $D$ contain $k$ spectra, e.g., taken as a sequence in time from a chemical reaction system. Each spectrum consists of $n$ absorbance values. The matrix $C \in \mathbb{R}^{k \times s}$ is the concentration factor, $A \in \mathbb{R}^{s \times n}$ is the spectra matrix and $s$ is the number of the chemical components. In general this factorization problem does not have a unique solution. Even if the factors are scaled in a certain way, there are usually many substantially different solutions. This is a

well-known phenomenon, which is called the rotational ambiguity of the solution [15]. We refer to the introduction of the first part of this paper [7] for a short introduction to the pure component factorization problem and for many references to the literature.

Due to their physical meaning the three matrices $D$, $C$ and $A$ should have only nonnegative components. However, for experimental and perturbed or noisy data the factors $C$ and $A$ can contain small negative components. Especially, if the spectral data in $D$ has undergone a background subtraction, then small negative entries can occur. Then it is often necessary to allow slightly negative entries in the factors $C$ and $A$ in order to find factors which approximate chemically meaningful solutions.

Our goal is to determine the set of all feasible factors $C$ and $A$ so that the product $CA$ reconstructs the given spectral data matrix $D$. Here we consider only three-component systems. For two- and four-component systems see the survey papers [12, 14] and [1, 5]. Borgen plots [3, 10] are geometric constructions which represent all nonnegative factorizations of $D$ for three-component systems by two-dimensional plots. The two coordinates of the points in the planar Borgen plots are the expansion coefficients of feasible solutions with respect to the basis of singular vectors of $D$. One of the three expansion coefficients for the three-component

systems is normalized to 1; this corresponds to a specific scaling of the solutions [7, 9].

The classical construction by Borgen and Kowalski [3] is limited to nonnegative data and results in nonnegative factorizations. However, Borgen plots suffer from their restriction to nonnegative data. In the first part of this paper [7] *generalized Borgen plots* have been introduced in order to overcome this limitation. The extended concept includes a geometric algorithm which allows to construct geometrically the area of feasible solutions (AFS). In the limiting case of vanishing negative entries in $D$, the generalized Borgen plots are equal to the classical Borgen plots.

In any case, Borgen plots and generalized Borgen plots provide a deeper understanding of the possible manifestations of the rotational ambiguity. These are uniqueness, partial uniqueness [11] up to high non-unique solutions. Such larger sets of feasible solutions may have the form of a single-set AFS and AFS sets consisting of three or even more isolated subsets [12].

## 1.1. Organization of this paper

Section 2 recapitulates the central definitions and main properties of the AFS and Borgen plots. These explanations depend decisively on the respective scaling, which is sometimes a normalization. Here we focus on the *first singular vector scaling* which is explained in [7], see also [9]. Section 3 is dedicated to the new *line-moving algorithm*. This algorithm generalizes the classical tangent algorithm of Borgen and Kowalski [3, 10]. This algorithm is also introduced briefly at the beginning of Section 3. Then the line-moving algorithm is described in detail. Many graphical illustrations support the explanations. The mathematical justification of the line-moving algorithm is given in Section 4. Numerical experiments in Section 5 conclude the paper.

## 1.2. Guideline for the reader

The reader who is familiar with the AFS and with the construction of the inner polygon (called INNPOL by Borgen and Kowalski [3]) and the outer polygon (called FIRPOL) may skip Section 2. The new line-moving algorithm and its numerical application are part of Sections 3 and 5. For readers who are mainly interested in the justification of the line-moving algorithm we suggest to focus on Section 4. However, this section is devoted to the mathematical analysis of the line-moving algorithm. The reader may skip this section if he is mainly interested in the construction of the line-moving algorithm and its applications.

## 1.3. Notation

The following notation is used in the paper. The references apply to the first usage of the symbol.

| | |
|---|---|
| $D \in \mathbb{R}^{k \times n}$ | spectral data matrix, see Sec. 1. |
| $C \in \mathbb{R}^{k \times 3}$ | concentration matrix, see Sec. 1. |
| $A \in \mathbb{R}^{3 \times n}$ | spectra matrix, see Sec. 1. |
| $U \Sigma V^T$ | truncated singular value decomposition of $D$, see Sec. 2. |
| $T \in \mathbb{R}^{3 \times 3}$ | transformation matrix, see Eq. (2). |
| $t \in \mathbb{R}^2$ | low-dimensional representation of spectra by $t = T(1, 2 : 3)$, see Def. 2.1. |
| $e \in \mathbb{R}^n$ | all-ones vector $(1, \dots, 1)^T$, see Sec. 2.2. |
| $\varepsilon_C$ | parameter which bounds negative entries in $C$, see Def. 2.1. |
| $\varepsilon_A$ | parameter which bounds negative entries in $A$, see Def. 2.1. |
| $\mathcal{M}_{\varepsilon_C, \varepsilon_A}$ | generalized AFS, see Def. 2.1. |
| $\Omega \in \mathbb{R}^{k \times k}$ | scaling matrix, see Eq. (3). |
| $\mathcal{I}$ | set of the vertices of INNPOL, see Sec. 3. |
| $\mathcal{I}_i$ | enumeration of the vertices of INNPOL, see Sec. 4. |
| $\mathcal{I}_{\mathcal{P}}$ | set of displaced vertices of INNPOL related to an initial point $P$ of FIRPOL, see Eq. (5). |
| $\mathcal{I}_Q$ | set of displaced vertices of INNPOL, related to an initial point $Q$ of FIRPOL, see Eq. (6). |

We use the colon notation in order to extract submatrices or vectors from a given matrix $A$. Thus $A(:, i)$ is the $i$th column of $A$ and $A(i, :)$ is the $i$th row. The vector $(\ell_1, \ell_1 + 1, \dots, \ell_2)$ of integer numbers is abbreviated by $\ell_1 : \ell_2$. The submatrix of $A$ containing its columns $\ell_1$ up to $\ell_2$ is $A(:, \ell_1 : \ell_2)$. Rows of $A$ can be extracted by swapping the arguments.

## 2. On almost nonnegative matrix factorizations

In the first part of this paper we have analyzed the nonnegative matrix factorization problem for $D$ and more general factorizations which allow small negative entries in the factors $C$ and $A$ for $s$-component systems [7]. Here, we consider only the case of three-component systems with $s = 3$ for the geometric construction of the AFS. This restriction also underlies the work of Borgen and Kowalski [3]. Geometric constructions of the AFS for four-component systems have not been developed so far.

Let $D$ be a $k$-by-$n$ spectral data matrix. We are interested in all factorizations $D = CA$ where the factors $C$ and $A$ are bounded from below elementwise

$$A \geq -\varepsilon_A \text{ and } \Omega C \geq -\varepsilon_C \qquad (1)$$

for small tolerance parameters $\varepsilon_A, \varepsilon_C \geq 0$, see Definition 2.1. The diagonal matrix $\Omega$ is introduced in Definition 2.1.

Any diagonal matrix $\Theta$ with positive diagonal elements together with its inverse can be inserted in the factorization. In this way $D = CA = (C\Theta^{-1})(\Theta A)$ results in rescaled solutions. However, these scaled solutions do not gain any new insight. Various scaling strategies, so-called Borgen norms have been suggested and tested [9].

In [7] the *row sum scaling (RS-scaling)* and *first right singular vector scaling (FSV-scaling)* play prominent roles. These scalings can be used even for data with small negative entries. The FSV-scaling is most commonly employed in the literature. We use this latter scaling for the following brief recapitulation of the important definitions and theorems. The proposed new line-moving algorithm can be formulated with each of these scalings.

## 2.1. Rotational ambiguity and the AFS

The starting point for a deeper study of the *rotational ambiguity* [15] is the truncated singular value decomposition (SVD) of $D$ [6]. The reduced SVD of a rank-3 matrix $D \in \mathbb{R}^{k \times n}$ reads $D = U\Sigma V^T$ with a diagonal matrix $\Sigma \in \mathbb{R}^{3 \times 3}$ and orthogonal $U \in \mathbb{R}^{k \times 3}$ and $V \in \mathbb{R}^{n \times 3}$. This factorization allows to represent all possible factorizations by inserting a regular matrix $T \in \mathbb{R}^{3 \times 3}$ and its inverse according to

$$D = \underbrace{U\Sigma T^{-1}}_{C} \underbrace{TV^T}_{A}. \qquad (2)$$

One is only interested in those matrices $T$ which result in nonnegative factors $C$ and $A$ or in factors which are almost nonnegative in the sense of the componentwise inequalities (1).

The AFS represents all possible factorizations (2) or equivalently all feasible matrices $T$. A permutation argument shows that it is sufficient to consider only all the first rows of feasible matrices $T$. And even more, the FSV-scaling [7] allows to fix the first entry $T(1,1)$ of this row to 1. Hence the first column of $T$ is the all-ones vector [7, 13]. The AFS is defined to be the set of all vectors $t = T(1, 2 : 3)$ which are connected to a regular matrix $T$ so that $C = U\Sigma T^{-1}$ and $A = TV^T$ are nonnegative matrices. These nonnegativity constraints
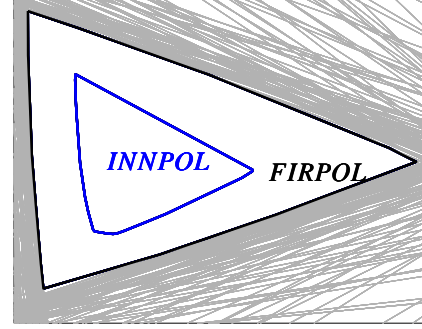


Figure 1: The polygons INNPOL and FIRPOL for the model problem introduced in Section 5.1. For the construction of FIRPOL the parameter $\varepsilon_A = 0.005$ has been used. The boundary of the half-planes defining FIRPOL are drawn by gray lines.

for $C$ and $A$ can be weakened by assuming the inequality (1). The resulting generalized AFS with respect to FSV-scaling is defined next.

**Definition 2.1.** *Let $D \in \mathbb{R}^{k \times n}$ be a rank-3 matrix, and let $D = U\Sigma V^T$ be the truncated SVD of $D$ with $U \in \mathbb{R}^{k \times 3}$, $\Sigma \in \mathbb{R}^{3 \times 3}$ and $V \in \mathbb{R}^{n \times 3}$. If the diagonal matrix $\Omega \in \mathbb{R}^{k \times k}$*

$$\Omega(i,i) = (U\Sigma)_{i,1}^{-1} \quad i = 1, \ldots, k, \qquad (3)$$

*has positive diagonal elements (see Sec. 3.4 in [7] for the justification and the construction of $\Omega$), then for parameters $\varepsilon_C \geq 0$ and $\varepsilon_A \geq 0$ the spectral factor AFS with respect to FSV-scaling is defined to be the set*

$$\mathcal{M}_{\varepsilon_C, \varepsilon_A} = \Big\{ t \in \mathbb{R}^{1 \times 2} : \text{ exists regular } T, T(1, :) = (1, t),$$
$$\Omega U\Sigma T^{-1} \geq -\varepsilon_C, TV^T \geq -\varepsilon_A \Big\}.$$

## 2.2. INNPOL, FIRPOL and the construction of the AFS

The AFS is a subset of a first polygon (FIRPOL), see Definition 2.3. The AFS lies outside the polygon (INN-POL), which is defined in Definition 2.2; see [3, 4, 10]. INNPOL is a subset of FIRPOL, see Figure 1, where these polygons are drawn for the spectral data matrix of the model problem from Section 5.1.

**Definition 2.2.** *The convex hull of the row vectors of $\Omega DV(:, 2 : 3)$ is called inner polygon (INNPOL). Therein $\Omega$ is given by Eq. (3).*

The polygon FIRPOL is defined by all coefficient vectors which result in nonnegative linear combinations of the right singular vectors [3]. This condition is weakened in the following, namely $A = TV^T \geq -\varepsilon_A$ is a componentwise lower bound on the matrix elements of

$A$ for a $\varepsilon_A \geq 0$. Together with the scaling condition $T(:, 1) = (1, 1, 1)^T$ the defining inequality is

$$\sum_{i=2}^{3} T(1, i)(V(:, i))^T \geq -V(:, 1)^T - \varepsilon_A e, \qquad (4)$$

where $e = (1, 1, \ldots, 1)^T \in \mathbb{R}^n$ is the all-ones vector. The set of row vectors $t = T(1, 2 : 3) \in \mathbb{R}^{1 \times 2}$ which satisfy Eq. (4) defines the polygon FIRPOL.

**Definition 2.3.** *Let $D^T D$ be an irreducible matrix. Then the polygon given by*

$$\left\{ t \in \mathbb{R}^{1 \times 2} : \sum_{i=2}^{3} t_{i-1}(V(:, i))^T \geq -(V(:, 1))^T - \varepsilon_A e \right\}$$

*is an intersection of k half-spaces and is called FIRPOL. Therein $t_1$ and $t_2$ are the two components of $t \in \mathbb{R}^{1 \times 2}$.*

The chemical meaning of the polygons FIRPOL and INNPOL is as follows: FIRPOL represents the set of almost nonnegative spectra of a chemical three-component system in the abstract space of expansion coefficients. Each point of FIRPOL represents a spectrum. Any point outside FIRPOL is chemically meaningless as the associated "spectrum" contains components which are smaller than $-\varepsilon_A$.

The vertices of the polygon INNPOL are the representatives of the rows of the spectral data matrix $D$ in the AFS plane. This explains why INNPOL should be contained in the triangle whose vertices represent the pure component spectra. If small perturbations are allowed, then INNPOL might slightly intersect the triangle of the pure component spectra. Figure 1 shows not only the polygons INNPOL and FIRPOL, but also the half-spaces by gray lines. The intersection of all these half-spaces equals FIRPOL. In the case of a spectral data matrix $D$ which includes small negative components, the parameter $\varepsilon_A$ has to be sufficiently large (so $-\varepsilon_A$ is sufficiently small) so that INNPOL is a subset of FIRPOL. This is fulfilled, if and only if the inequality $\min(\Omega D V) \geq -\varepsilon_A$ holds. Then the AFS is a subset of FIRPOL and is also located outside INNPOL; this is the content of the next theorem.

**Theorem 2.4.** *The three points $T(i, 2 : 3)$, $i = 1, 2, 3$, in FIRPOL determine the existence of a* nonnegative *matrix factorization (case I) or the existence of a nearly nonnegative matrix factorization which can include small negative components (case II).*

*I: Let $D$ be a nonnegative matrix. Then $D = CA$ is a nonnegative matrix factorization with an FSV-scaled factor $A$ if and only if for the three points*
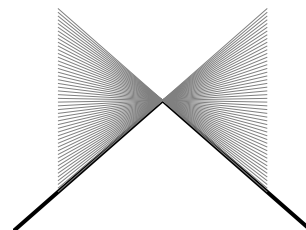


Figure 2: Family of tangent lines (gray lines) at a vertex of a convex polygon (black bold lines).

*$t^{(\ell)} \in \mathbb{R}^{1 \times 2}$ in FIRPOL with $A = T V^T$ and $T(\ell, 2 : 3) = t^{(\ell)}$ for $\ell = 1, 2, 3$ the convex hull of these three points includes the polygon INNPOL.*

*II: Let $D$ be a matrix, which fulfills the component-wise inequality $\Omega D \geq -\varepsilon_A$ for a proper $\varepsilon_A \geq 0$. The diagonal matrix $\Omega$ is given by Eq. (3). Then $D = CA$ is a matrix factorization with $\Omega C \geq -\varepsilon_C$ and $A \geq -\varepsilon_A$ with an FSV-scaled factor $A$ if and only if for three points $t^{(\ell)} \in \mathbb{R}^{1 \times 2}$ in FIRPOL with $A = T V^T$ and $T(\ell, 2 : 3) = t^{(\ell)}$ for $\ell = 1, 2, 3$ the affine hull of these three points $t^{(\ell)}$ includes INN-POL. All the expansion coefficients of the affine linear combinations are greater than or equal to $-\varepsilon_C$.*

The proof of case I is part of the classical analysis of Borgen and Kowalski [3]. Case II is proved by Theorem 3.11 in the first part of this paper [7]. Theorem 2.4 describes the core idea of the (illustrative) geometric interpretation of the AFS: By construction each point of the AFS is a vertex of a certain triangle in FIRPOL so that each of the vertices of INNPOL can be represented by an affine combination of the vertices of this triangle. The expansion coefficients in these affine combinations are all greater than or equal to $-\varepsilon_A$. An example is shown in Figure 3 where the three vertices $P$, $Q$ and $R$ belong to the AFS since the triangle includes INNPOL and is included in FIRPOL.

## 3. The line-moving algorithm

This section introduces the new line-moving algorithm for the geometric construction of generalized Borgen plots. The detailed justification of the algorithm is not included in this section, but postponed to Section 4.

First, we describe the tangent algorithm by Borgen and Kowalski [3]. The tangent algorithm and the *simplex rotation algorithm*, see also [3], allow to construct the AFS for the nonnegative matrix factorization problem with $\varepsilon_C = \varepsilon_A = 0$.
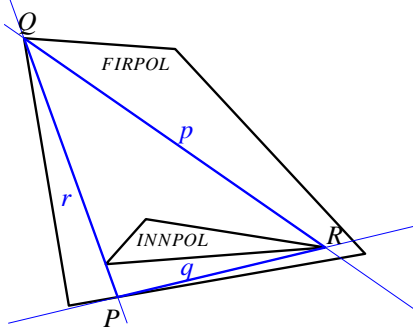
Figure 3: The tangent algorithm of Borgen and Kowalski to construct the so-called Borgen plots. Starting from a tangent line *r* to INNPOL, a triangle *PQR* is constructed so that each edge is a tangent to INNPOL. The point *R* belongs to the boundary of the AFS.

## 3.1. The tangent algorithm

According to Theorem 2.4, the key construction principle of the tangent algorithm is to find triangles within FIRPOL which enclose INNPOL. This relation between a factorization of $D$ and a triangle within FIRPOL is stated in case I of Theorem 2.4. Later, in Section 3.2 the line-moving algorithm generalizes the tangent algorithm by constructing triplets of points according to case II of Theorem 2.4.

Next we explain precisely the meaning of tangents at a vertex of a convex polygon. A tangent line at a boundary point of a polygon is uniquely defined as far as this boundary point is not a vertex. In a vertex the boundary curve of the polygon is not a differentiable function. For the general case the following definition holds.

**Definition 3.1.** *A tangent of a convex polygon is a straight line which touches the polygon in at least one point and which does not intersect the interior of the polygon.*

Hence, at a vertex a family of possible tangent lines exists. This is illustrated by Figure 2.

The tangent algorithm [2, 3, 10] works as follows: We start with a tangent line *r* to the inner polygon; see Figure 3 for an illustration of the following steps.

1. A tangent line *r* of INNPOL intersects FIRPOL at the points *P* and *Q*.

2. Construct the second tangent line *q* to INNPOL starting in *P*.

3. Construct the third tangent line *p* to INNPOL starting in *Q*.

4. The point of intersection of *q* and *p* is *R*.

5. If *R* is inside FIRPOL and the triangle *PQR* encloses INNPOL, then *R* belongs to the boundary of the AFS. If *PQR* does not enclose INNPOL, then the point *R* is meaningless; proceed with step 6.

6. Rotate the initial tangent *r* around INNPOL (in order to construct all possible tangents to INNPOL) and repeat the construction with step 1.

The set of all points *R* which result from the tangent rotation algorithm belongs to the AFS according to Theorem 2.4. These points constitute a major part of the boundary of the AFS. These parts of the boundary are drawn by bold black lines in Figure 11. The remaining parts of the boundary of the AFS belong to the boundary of FIRPOL or are connecting lines between these two types of boundaries. It can be proven that *R* is never an interior point of the AFS but belongs to the boundary. Otherwise, the line *p* would not be tangent at INNPOL so that *R* can be moved to the inside of the initial triangle *PQR*. Numerically, the tangent line *r* is rotated around INNPOL where the possible angle values, which determine the slope of this tangent, are taken from a certain discretization of the angle interval $[0, 360)$ measured in degrees. The following line-moving algorithm generalizes the classical tangent algorithm.

## 3.2. The line-moving algorithm

This section provides the recipe how to construct the AFS $\mathcal{M}_{\varepsilon_C, \varepsilon_A}$. The mathematical justification of the algorithm is provided in Section 4. The procedure is similar to the tangent algorithm. The construction starts with a tangent line *r* at INNPOL. First an auxiliary point *H* is constructed. The geometry underlying Procedure I is illustrated by Figure 4.

***Procedure I**: Construction of the auxiliary point H.*

1. For a tangent line *r* to INNPOL the points of intersection *P* and *Q* with FIRPOL are determined.

2. Construct the tangent *q* to INNPOL through *P*.

3. Construct the tangent *p* to INNPOL through *Q*.

4. The intersection of *q* and *p* is *H*.

5. If the triangle *PQH* does not enclose INNPOL, then *H* is mirrored along *r*. Otherwise *H* is not changed.

If *H* is inside FIRPOL and has not been flipped along *r*, then the point *H* belongs to the AFS of nonnegative factorizations by construction. However, *H* is not a point on the boundary of the AFS if $\varepsilon_C > 0$, cf. Theorem 4.6. The point *H* defines the search direction in the following "Procedure II".
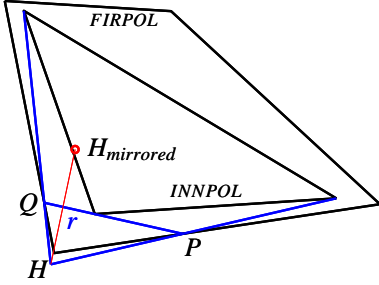
5

Figure 4: Construction of the auxiliary point $H$ for the line-moving algorithm. If the triangle $PQH$ does not enclose INNPOL, then the point $H$ is mirrored along $r$. The mirrored point $H$ is used to define a search direction in the algorithm.

The line-moving algorithm constructs the AFS not by tangent lines to INNPOL (as the tangent algorithm), but by tangents to certain displacements of the polygon INNPOL. If $\mathcal{I}$ denotes the polygon INNPOL, then we need the two displacements $\mathcal{I}_P$ and $\mathcal{I}_Q$ of INNPOL. These are given by

$$\mathcal{I}_P = \left\{ \frac{S + \varepsilon_C P}{1 + \varepsilon_C} : S \in \mathcal{I} \right\}, \tag{5}$$

$$\mathcal{I}_Q = \left\{ \frac{S + \varepsilon_C Q}{1 + \varepsilon_C} : S \in \mathcal{I} \right\}. \tag{6}$$

Therein the variable $S$ runs through all vertices of INN-POL. In words, the set $\mathcal{I}_P$ results from adding $\varepsilon_C P$ to each point of INNPOL and by subsequent multiplication of the resulting vector by $1/(1 + \varepsilon_C)$. The set $\mathcal{I}_Q$ is a similar displacement of $\mathcal{I}$. The line-moving algorithm requires that the sets $\mathcal{I}_P$ and $\mathcal{I}_Q$ are updated for each line $PQ$. The indexes $P$ and $Q$ of these sets symbolize the dependency on the points $P$ and $Q$.

Then from $P, Q, \mathcal{I}_P$ and $\mathcal{I}_Q$ a point $R$ is constructed. This point $R$ is the intersection of the two tangents to $\mathcal{I}_P$ and to $\mathcal{I}_Q$, see Figure 5 for an illustration. With these points each vertex of INNPOL is an affine combination of $P$, $Q$ and $R$ and the linear coefficients of $P$ and $Q$ in the affine combination are greater than or equal to $-\varepsilon_C$, see Theorem 2.4. (The proof of this fact is given later in and after Theorem 4.6 in Section 4.) These steps are summarized in the next procedure.

***Procedure II**: Construction of the point R.*

1. Compute the sets $\mathcal{I}_P$ and $\mathcal{I}_Q$.
2. Construct the tangent line $q$ to $\mathcal{I}_Q$ through $P$. The point of tangency is to be determined in the same

half-plane (which results from the division of the plane by $r$) in which the point $H$ is located.

3. Construct the tangent line $p$ to $\mathcal{I}_P$ through $Q$. Again the point of tangency is to be determined in the half plane (with respect to $r$) which contains $H$.

4. The point of intersection of $q$ and $p$ is $R$.

5. Check whether $R$ is in FIRPOL.

The point $R$ belongs to the generalized AFS if it is inside FIRPOL; the mathematical justification is provided later in Theorem 4.6.

The line $PQ$ touches but does not intersect INNPOL. Next we move the line $r$ by a parallel shift into the two possible directions, namely either towards the interior of INNPOL or away from INNPOL. First we move $r$ towards INNPOL so that $r$ intersects INNPOL. The new points of intersection of $r$ with FIRPOL are denoted, once again, by $P$ and $Q$. The auxiliary point $H$ is not changed. As described above we compute the two sets $\mathcal{I}_P$ and $\mathcal{I}_Q$ and the point $R$. Figure 6 illustrates these steps. The shift increment of these parallel shifts of $r$ is denoted by $\delta d$. This parallel translation can be stopped if the construction cannot find a point of the AFS. Then $r$ is moved away from INNPOL, until $r$ leaves FIRPOL.

If $r$ does not intersect INNPOL and $R$ has successfully been constructed so that $R$ is in FIRPOL, then $R$ belongs to the AFS, see Theorem 4.6. If $r$ intersects INNPOL, then the expansion coefficients of the affine combinations which express the vertices of INNPOL in terms of $P$, $Q$ and $R$ are partially negative. In this case one has to check, whether or not $R$ belongs to the AFS. If $R$ is outside the polygon FIRPOL, then $R$ can be neglected. Otherwise, one has to check whether or not all vertices of INNPOL are affine combinations of $P$, $Q$ and $R$ and the linear coefficients of $R$ are greater than or equal to $-\varepsilon_C$, see Theorem 2.4. If this condition for the affine combination condition is fulfilled, then $R$ belongs to the AFS. Further, the convex polygon, which is limited by the boundary of FIRPOL and the two lines passing through either $P$ and $R$ or $Q$ and $R$, belongs to the AFS, e.g. the blue filled polygon in Figure 5.

If $R$ is inside FIRPOL but the affine combination condition is not fulfilled, then we search for points of the AFS which are located on the lines passing through $P$ and $R$ or through $Q$ and $R$. The justification for this is given later in Theorem 4.6. Therefore we compute the point of intersection $R_1$ of the line through $P$ and $R$ with the boundary of FIRPOL. If all vertices of INN-POL fulfill the affine combination condition for $P$, $Q$ and $R_1$, then $R_1$ belongs to the AFS. Now, by using the
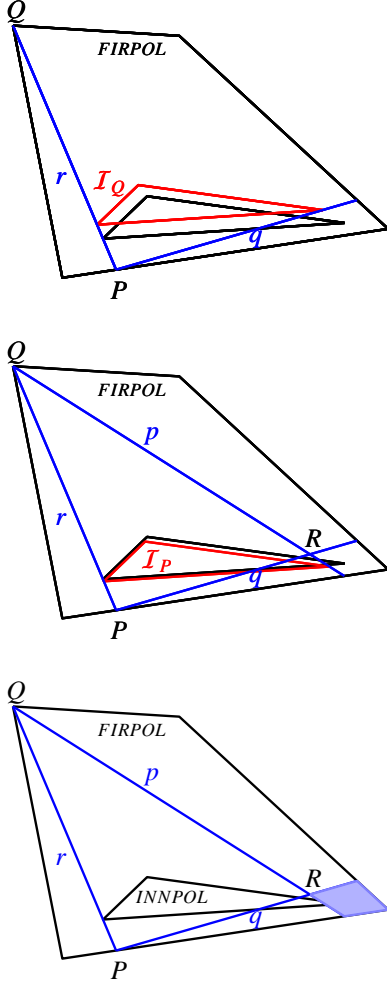
Figure 6: Computation of a part of the AFS by parallel translation of the line $r$ towards the center of INNPOL. The blue filled polygon belongs to the AFS. The points $R_1^0$ and $R_2^0$ are constructed as described in Procedure III.

bisection method, one can find the point $R_1^0$ on the same line which is closest to $R$ and still fulfills the affine combination condition. Then the convex polygon, which is limited by the boundary of FIRPOL, the line passing through $R_1^0$ and $P$ and also the line through $R_1^0$ and $Q$, belongs to the AFS. In the same way the point $R_2$ is computed as the point of intersection of FIRPOL with the line passing through $Q$ and $R$. If $R_2$ belongs to the AFS, then we compute the point $R_2^0$ which is closest to $R$ on the line through $R$ and $Q$ and which belongs to the AFS.

A short summary of this step of the algorithm is as follows:

**Procedure III**: *Computation of $R_1^0$ and $R_2^0$.*

- If $R$ is outside FIRPOL, then neglect R.
- Else if $R$ does not belong to the AFS, then compute the two points $R_1$ and $R_2$ of intersection of $p$ and $q$ with the boundary of FIRPOL.

    - If $R_1$ belongs to the AFS, then compute $R_1^0$.
    - If $R_2$ belongs to the AFS, then compute $R_2^0$.

After the line $r$ has been shifted parallel to maximal distances into the two possible directions away from its initial position, then the rotation process of $r$ around INNPOL is continued. The discrete numerical process requires that $r$ is rotated by a fixed small angle increment $\delta\phi$. After rotation of $r$, the points $P$ and $Q$ are recomputed and the point $H$ is to be updated.

Algorithm 1 combines the three procedures I-III with the tangent rotation process. The required input data are the two polygons FIRPOL and INNPOL, the shift increment parameter $\delta d$ (which is determined by $\varepsilon_C$) and the rotation angle increment $\delta\phi$. An illustration of the line-moving algorithm is given in Figure 7.



Figure 5: Construction of the point $R$ by the line-moving algorithm. Top: The initial tangent $r$ to INNPOL, the displacement $\mathcal{I}_Q$ of INNPOL and the tangent $q$ to the set $\mathcal{I}_Q$. Center: The second tangent $p$ to the displacement $\mathcal{I}_P$ of INNPOL is constructed. Bottom: The point $R$ is the intersection of $p$ and $q$ and belongs to the generalized AFS $\mathcal{M}_{\varepsilon_C,\varepsilon_A}$. The further computation shows that the complete blue filled polygon belongs to the AFS.
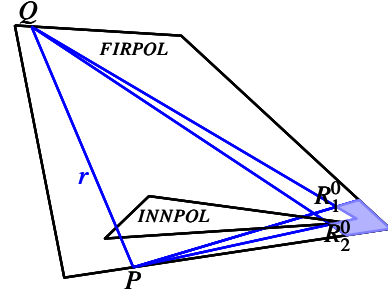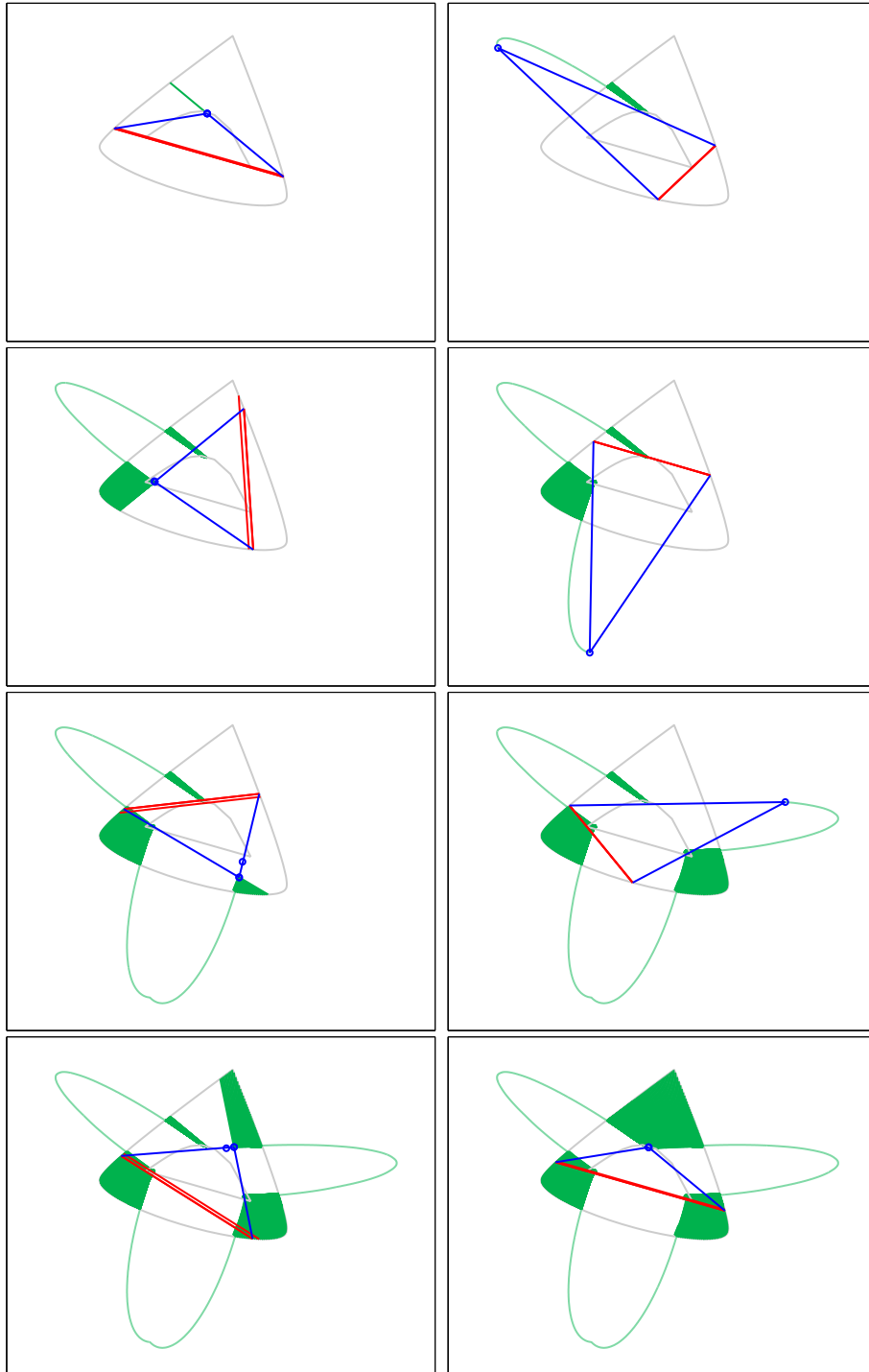
Figure 7: Illustration of the AFS construction by the line-moving algorithm from the starting stage (left uppermost subfigure) until completion (right lowermost subfigure). The closely adjacent two red lines are the innermost and outermost lines which are used by the algorithm. For the inner red tangent line the two blue lines start at the points of intersection with FIRPOL. The blue lines are tangents at the sets $\mathcal{I}_P$ respectively $\mathcal{I}_Q$. The point of intersection of these two blue lines belongs to the AFS if it is contained in FIRPOL. The two blue dots (the second blue dot is constructed by the second red line in the same way) represent the innermost and outermost AFS points which are constructed from the lines parallel to the red lines. The green areas inside FIRPOL belong to the AFS; these areas are growing in the AFS construction process. The last subfigure shows the final AFS.

8

**Algorithm 1** The line-moving algorithm

**Require:** INNPOL, FIRPOL, $\delta d$ and $\delta\phi$.

  Construct initial tangent $r$ to INNPOL

  $l$ = smallest integer larger than $360/\delta\phi$

  **for** $i = 1 : l$ **do**

     Rotate tangent line $r$ around INNPOL by the
       rotation angle increment $\delta\phi$ (in degrees).

     *Procedure I* $\rightarrow$ compute $H$

     *Procedure II* $\rightarrow$ compute $R$

     **while** $R$, $R_1^0$ or $R_2^0$ belongs to the AFS **do**

        move $r$ parallel towards center of INNPOL
          (the parallel shift increment is $\delta d$).

        *Procedure II* $\rightarrow$ compute $R$

        **if** $R$ is in FIRPOL, $R$ is not in the AFS **then**

          *Procedure III* $\rightarrow$ compute $R_1^0, R_2^0$.

        **end if**

     **end while**

     **while** $r$ intersects FIRPOL **do**

        move $r$ parallel away from INNPOL
          (the parallel shift increment is $\delta d$).

        *Procedure II* $\rightarrow$ compute $R$

     **end while**

  **end for**

### 3.3. Parameter selection in the line-moving algorithm

The line-moving algorithm needs four parameters to be defined. The two parameters $\varepsilon_C$ and $\varepsilon_A$ have a direct impact on the AFS as they limit the acceptable size of negative entries in the factors $C$ and $A$, see Eq. (1). For $\varepsilon_A$ the inequality $\Omega D \geq -\varepsilon_A$ has to be fulfilled so that the inner polygon INNPOL is still contained in the polygon FIRPOL. If the limit $\min(\Omega D) = -\varepsilon_A$ is attained, then a vertex of INNPOL is located on the boundary of FIRPOL. In order to stabilize the numerical computation one should choose $\varepsilon_A$ slightly greater than this minimum. We found $\varepsilon_A = -1.05 \min(\Omega D)$ to be a good choice for many AFS computations for perturbed data. The parameter $\varepsilon_C$ limits the acceptable size of negative entries in the factor $C$. An increasing value of $\varepsilon_C$ increases the size of the AFS and the computation time. Hence $\varepsilon_C$ should be as small as possible, but the parameter must be increased with an increasing noise level. In general, by increasing $\varepsilon_A$ or $\varepsilon_C$ the size of the AFS increases, see Lemma 3.12 in [7]. The geometric AFS construction works well for data with relatively small perturbations. Moreover, the algorithm is more stable if the negative entries are mainly concentrated in the factor $A$.

The parameters $\delta d$ and $\delta\phi$ influence the accuracy and computation time of the algorithm. The distance between the parallel lines in FIRPOL from which the points $R$ of the AFS are computed is given by $\delta d$. The smaller the value of $\delta d$, the greater the accuracy and the computation time. The parameter $\delta\phi$ is the rotation angle of the lines $PQ$ in the line-moving algorithm. This control parameter influences the accuracy and computation time in a similar way as $\delta d$. The smaller the value of $\delta\phi$, the greater are the accuracy and the computation time. Tables 1 and 2 demonstrate these relations for the three-component model problem presented in Section 5.1.

### 3.4. Implementation in the FACPACKsoftware

The line-moving algorithm is implemented in the *Generalized Borgen plot module* of the *FACPACK* software. This software and a tutorial can be accessed at

http://www.math.uni-rostock.de/facpack/

*FACPACK* allows to construct the generalized Borgen plots with respect to the RS-scaling and alternatively with the FSV-scaling. The parameters for $\varepsilon_C$ and $\varepsilon_A$ can be modified. It is also possible to change the parallel shift increment $\delta d$ and the rotation angle increment $\delta\phi$. By a *live-view mode* the AFS can be explored interactively. While the mouse pointer is moved through the AFS the related spectra or profiles are displayed. Certain spectra or concentration profiles can be fixed and a reduced AFS can be computed. This smaller AFS takes into account this additional knowledge on the pure component factorization.

## 4. Justification of the line-moving algorithm

According to Theorem 2.4 feasible points in AFS are associated with triangles in FIRPOL. The line-moving algorithm works with the premise that for a construction of the boundary of the AFS always two vertices of the triangles can be fixed to the boundary of FIRPOL. Further, the edges of these triangles can be assumed to be tangents to the sets $\mathcal{I}_P$ or $\mathcal{I}_Q$; see Equations (5) and (6). This section provides a justification for these assumptions. First we show that it is possible to construct the AFS starting from points $P$ and $Q$ located on the boundary of FIRPOL.

**Lemma 4.1.** *For each point R inside the AFS there exist two points P and Q so that all vertices of INNPOL are affine combinations of P, Q and R with expansion coefficients greater than or equal to $-\varepsilon_C$.*

*It is possible to choose at least one of the points P and Q to be located on the boundary of FIRPOL.*
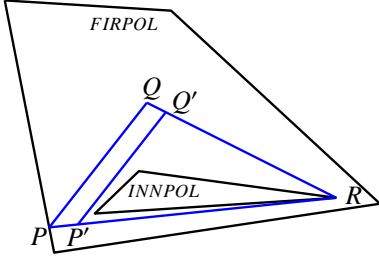
Figure 8: Illustration of the idea of the proof of Lemma 4.1. For each point $R$ in the AFS there exist two points $P$ and $Q$ so that the affine hull of $P$, $Q$ and $R$ encloses INNPOL and where the affine hull includes only expansion coefficients greater than or equal to $-\varepsilon_C$. By stretching the triangle $P'Q'R$ with fixed $R$ at least one of the points $P'$ and $Q'$ is moved to the boundary of FIRPOL.
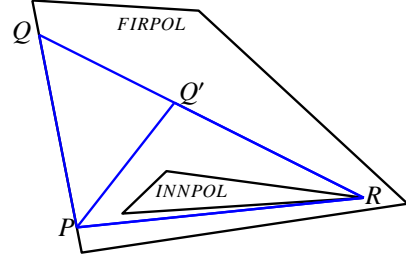


Figure 9: Illustration of Theorem 4.2. For each point $R$ of the AFS there exist two points $P$ and $Q$ so that the affine hull of $P$, $Q$ and $R$ with expansion coefficients greater than or equal to $-\varepsilon_C$ encloses INNPOL. $P$ and $Q$ can be located on the boundary of FIRPOL.

*Proof.* Let $\mathcal{I}_1, \mathcal{I}_2, \ldots$ be an enumeration of the finite number of vertices of the polygon INNPOL $\mathcal{I}$. Taking an arbitrary vertex $\mathcal{I}_i$, then this point is an affine combination of $R$ and two additional points $P'$ and $Q'$, i.e.

$$\mathcal{I}_i = \alpha_i P' + \beta_i Q' + \gamma_i R. \qquad (7)$$

For this affine combination Theorem 2.4 guarantees $\alpha_i \geq -\varepsilon_C, \beta_i \geq -\varepsilon_C, \gamma_i \geq -\varepsilon_C$ and $\alpha_i + \beta_i + \gamma_i = 1$.

Next we consider a point $P$ so that $P'$ is a convex combination of $P$ and $R$, i.e. $P' = \lambda P + (1 - \lambda)R$ for $\lambda \in [0, 1]$. We also consider a point $Q$ so that $Q' = \lambda Q + (1 - \lambda)R$ with the same $\lambda$. Inserting these two convex combinations in (7) results in

$$\begin{aligned} \mathcal{I}_i =& \alpha_i(\lambda P + (1 - \lambda)R) + \beta_i(\lambda Q + (1 - \lambda)R) + \gamma_i R \\ =& \alpha_i \lambda P + \beta_i \lambda Q + (\alpha_i(1 - \lambda) + \beta_i(1 - \lambda) + \gamma_i) R. \end{aligned}$$

This geometry is illustrated by Figure 8. For this representation of $\mathcal{I}_i$ in terms of $P$, $Q$ and $R$ the sum of coefficients is equal to 1 since

$$\alpha_i \lambda + \beta_i \lambda + \alpha_i(1 - \lambda) + \beta_i(1 - \lambda) + \gamma_i = \alpha_i + \beta_i + \gamma_i = 1.$$

For the expansion coefficients of the linear combination it holds that $\beta_i \lambda \geq -\varepsilon_C, \gamma_i \lambda \geq -\varepsilon_C$ and

$$\begin{aligned} \alpha_i(1 - \lambda) + \beta_i(1 - \lambda) + \gamma_i = \underbrace{\alpha_i + \beta_i + \gamma_i}_{=1} - \lambda \underbrace{(\alpha_i + \beta_i)}_{=1-\gamma_i} \\ = 1 - \lambda + \lambda \gamma_i \geq \lambda \gamma_i \geq -\varepsilon_C. \end{aligned}$$

This proves that $\mathcal{I}_i$ is also an affine combination of $P$, $Q$ and $R$ with linear coefficients greater than or equal to

$-\varepsilon_C$. Geometrically, we have analyzed a stretching of the triangle. The triangle $PQR$ is similar to the triangle $P'Q'R$, and the triangle $P'Q'R$ can be stretched with a fixed-point in $R$ until (at least) one of the points $P$ and $Q$ is located on the boundary of FIRPOL. This completes the proof.

$\square$

The next theorem shows that $P$ together with $Q$ can be located on the boundary of FIRPOL.

**Theorem 4.2.** *For each point $R$ in the AFS there exist two points $P$ and $Q$ on the boundary of FIRPOL so that all vertices of INNPOL are affine combinations of $P$, $Q$ and $R$ with linear coefficients greater than or equal to $-\varepsilon_C$.*

*Proof.* By Lemma 4.1 for any point $R$ in the AFS there exist two other points $P$ and $Q'$ in the AFS so that at least one of the points, say $P$, is located on the boundary of FIRPOL, and each vertex of INNPOL is a feasible affine combination of $P$, $Q'$ and $R$. Suppose that $Q'$ is not on the boundary of FIRPOL. Then a ray starting in $R$ and passing through $Q'$ intersects FIRPOL in $Q$, see Figure 9. The point $Q'$ is a convex combination of $Q$ and $R$

$$Q' = \lambda Q + (1 - \lambda)R$$

with $0 < \lambda < 1$. Let $\mathcal{I}_i$ be the $i$th vertex of INNPOL. Then the following relation holds

$$\begin{aligned} \mathcal{I}_i =& \alpha_i P + \beta_i Q' + \gamma_i R \\ =& \alpha_i P + \beta_i(\lambda Q + (1 - \lambda)R) + \gamma_i R \\ =& \alpha_i P + \beta_i \lambda Q + (\gamma_i + \beta_i(1 - \lambda))R \end{aligned}$$
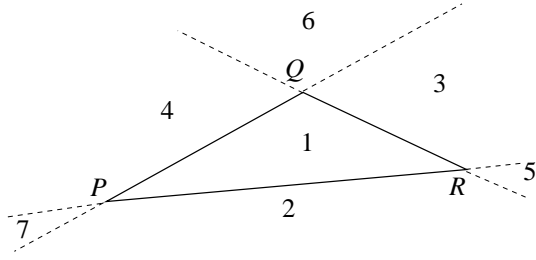
10

Figure 10: Signs of the barycentric coordinates in a triangle.

with $\alpha_i, \beta_i, \gamma_i \geq -\varepsilon_C$ and $\alpha_i + \beta_i + \gamma_i = 1$.

Let us suppose that the coefficient of $R$ breaks the $-\varepsilon_C$ bound, i.e. $\gamma_i + \beta_i(1 - \lambda) < -\varepsilon_C$. Next we derive a contradiction. The inequality implies that $\beta_i$ as well as $\gamma_i$ must then be negative. The negative coefficient $\gamma_i$ of $R$ means that $\mathcal{I}_i$ belongs to the half-plane which is on the other side of the line $PQ'$ than the point $R$, cf. Remark 4.3. Simultaneously, a negative coefficient $\beta_i$ of $Q'$ means that $\mathcal{I}_i$ belongs to the half-plane which is on the other side of the line $PR$ than the point $Q$.

This means that $\mathcal{I}_i$ is outside FIRPOL, since $P$ is on the boundary of FIRPOL. Therefore $\mathcal{I}_i$ is not a vertex of INNPOL. This is a contradiction so that $\gamma_i + \beta_i(1 - \lambda) \geq -\varepsilon_C$ must be true.

This proves that all vertices of INNPOL are each affine combinations of $P$, $Q$ and $R$ with expansion coefficients greater than or equal to $-\varepsilon_C$. $\qquad\square$

**Remark 4.3.** *The barycentric coordinate of the point*

$$\alpha P + \beta Q + \gamma R$$

*in the triangle PQR is the triplet $(\alpha, \beta, \gamma)$ with $\alpha \geq 0$, $\beta \geq 0$, $\gamma \geq 0$ and $\alpha + \beta + \gamma = 1$. All points in area 1 in Figure 10 can be addressed in this way. If negative barycentric coordinates $\alpha$, $\beta$ and $\gamma$ are allowed and $\alpha + \beta + \gamma = 1$ is still assumed to hold, then the (generalized) barycentric coordinates in the areas 2 up to 7 in Figure 10 satisfy the following sign conditions:*

| | |
|---|---|
| 2 | $\alpha \geq 0, \ \beta \leq 0, \ \gamma \geq 0,$ |
| 3 | $\alpha \leq 0, \ \beta \geq 0, \ \gamma \geq 0,$ |
| 4 | $\alpha \geq 0, \ \beta \geq 0, \ \gamma \leq 0,$ |
| 5 | $\alpha \leq 0, \ \beta \leq 0, \ \gamma \geq 0,$ |
| 6 | $\alpha \leq 0, \ \beta \geq 0, \ \gamma \leq 0,$ |
| 7 | $\alpha \geq 0, \ \beta \leq 0, \ \gamma \leq 0.$ |

Theorem 4.2 guarantees that the construction of the full AFS is possible starting from the points $P$ and $Q$ on

the boundary of FIRPOL. These points on the boundary of FIRPOL are said to belong to the *outer boundary* of the AFS. The key idea of the tangent algorithm and of the line-moving algorithm is to construct all points on the *inner boundary* of the AFS.

**Definition 4.4** (Inner and outer boundary of the AFS)**.**
*A point $R$ belongs to the inner boundary of the AFS, if for all triangles PQR, whose affine hull with expansion coefficients greater than or equal to $-\varepsilon_C$ includes INN-POL, there is no point $R'$ inside PQR, such that INN-POL is enclosed in the affine hull of PQR' with expansion coefficients greater than or equal to $-\varepsilon_C$.*
*The outer boundary of the AFS is given by the intersection of the AFS with the boundary of the polygon FIR-POL.*

It is possible that a certain point can belong to the inner and to the outer boundary of the AFS simultaneously. Surprisingly, it is also possible that points on the boundary of the AFS belong neither to the inner nor to the outer boundary. An example is shown and explained in Figure 11. Then the remaining parts of the boundary of the AFS are constructed by connecting the endpoints of the inner boundary with the associated endpoints of the outer boundary by straight lines, as illustrated by the blue polygons in Figures 5 and 6. The points on the inner boundary of the AFS (and sometimes interior points of the AFS) are constructed by tangent lines to the sets $\mathcal{I}_P$ and $\mathcal{I}_Q$, see Equations 5 and 6.

**Lemma 4.5.** *Let $R$ be a point of the inner boundary of the AFS with additional two points $P$ and $Q$ on the boundary of FIRPOL such that INNPOL is enclosed in the affine hull of $P$, $Q$ and $R$ with expansion coefficients greater than or equal to $-\varepsilon_C$. Then for at least one vertex of INNPOL at least one expansion coefficient of the affine combination of this vertex in terms of $P$, $Q$ and $R$ is equal to $-\varepsilon_C$.*

*Proof.* Let $\mathcal{I}_i$ be the enumeration of the vertices of INN-POL. If $PQR$ is a triangle in FIRPOL, whose affine hull with expansion coefficients greater than or equal to $-\varepsilon_C$ encloses INNPOL, then each $\mathcal{I}_i \in \mathcal{I}$ is an affine combination of $P$, $Q$ and $R$. This reads

$$\mathcal{I}_i = \alpha_i P + \beta_i Q + \gamma_i R$$

with $\alpha_i + \beta_i + \gamma_i = 1$ and $\alpha_i, \beta_i, \gamma_i \geq -\varepsilon_C$. Suppose that the strict inequality $\alpha_i, \beta_i, \gamma_i > -\varepsilon_C$ would hold for each vertex of INNPOL. Let $R'$ be a convex combination of $P$, $Q$ and $R$ given by

$$R' = \lambda P + \lambda Q + (1 - 2\lambda)R$$

with $0 < \lambda < 0.5$. Then $R$ can be expressed as

$$R = \frac{R' - \lambda P - \lambda Q}{1 - 2\lambda}.$$

The vertices $\mathcal{I}_i$ of INNPOL can be rewritten as affine combinations of $P$, $Q$ and $R'$ so that

$$\mathcal{I}_i = \left(\alpha_i - \frac{\lambda\gamma_i}{1-2\lambda}\right)P + \left(\beta_i - \frac{\lambda\gamma_i}{1-2\lambda}\right)Q + \frac{\gamma_i}{1-2\lambda}R'.$$

The three coefficients in this representation of $\mathcal{I}_i$ can be decreased so that for a sufficiently small $\lambda_0$ the three inequalities

$$\left(\alpha_i - \frac{\lambda_0\gamma_i}{1-2\lambda_o}\right) \geq -\varepsilon_C, \qquad (8)$$

$$\left(\beta_i - \frac{\lambda_0\gamma_i}{1-2\lambda_0}\right) \geq -\varepsilon_C, \qquad (9)$$

$$\frac{\gamma_i}{1-2\lambda_0} \geq -\varepsilon_C \qquad (10)$$

hold and that equality is attained for at least one of the three inequalities. In order to verify this we consider the three possible cases $\gamma_i > 0$, $\gamma_i < 0$ or $\gamma_i = 0$. First, for $\gamma_i > 0$ a positive quantity is subtracted from $\alpha_i$ in (8) and also $\beta_i$ in (9). This allows to attain equality for a sufficiently large $\lambda_0$. If $\gamma_i < 0$, then equality can be attained in (10) for a sufficiently large $\lambda_0$. Finally, the case $\gamma_i = 0$ means that the vertex $\mathcal{I}_i$ is located on the line through $P$ and $Q$ so that the construction of $R'$ is not meaningful.

All this means that $R'$ belongs to the AFS and that $R$ is not a point on the inner boundary as a smaller triangle $PQR'$ has been constructed with $R'$ closer to INNPOL. $\qquad \square$

The following theorem provides the justification that the boundary of the AFS can be constructed only from the points of the AFS which result from a certain tangent construction to INNPOL. Subsequent to this theorem the geometric AFS construction with respect to the shifted sets $\mathcal{I}_P$ and $\mathcal{I}_Q$ is justified.

**Theorem 4.6.** *Let R be a point on the inner boundary of the AFS and let the points P and Q be on the boundary of FIRPOL so that INNPOL is enclosed in the affine hull of P, Q and R with expansion coefficients greater than or equal to $-\varepsilon_C$. Then for at least two of the points P, Q and R there exists (at least) one vertex of INNPOL so that the expansion coefficients of the affine combination being associated with these two points are equal to $-\varepsilon_C$.*
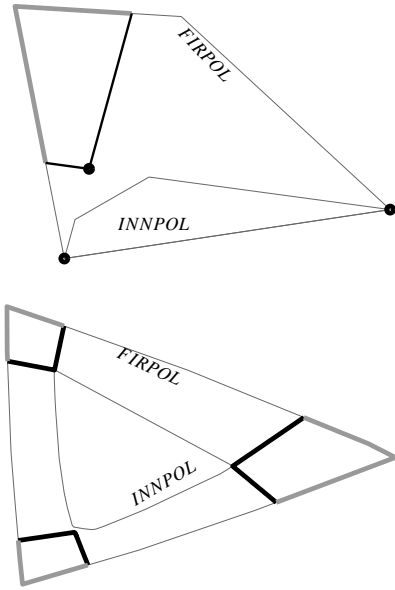


Figure 11: Top: One edge of INNPOL coincides with an edge of FIRPOL. For $\varepsilon_C = 0$ the inner boundary of the AFS consists of the three points marked by bold black dots. The outer boundary is given by the bold gray line. The remaining part of the boundary of the AFS does neither belong to the inner boundary nor to the outer boundary. Bottom: The inner boundary is given by the bold black lines and the inner boundary by the bold gray lines.
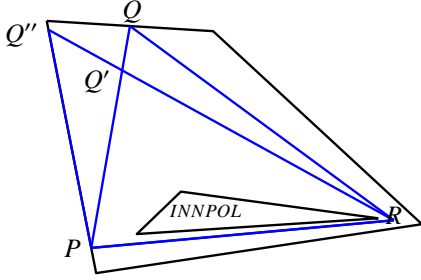
Figure 12: A typical geometry underlying the idea of the proof of Theorem 4.6.

*Proof.* Let $\mathcal{I}_i$ be an enumeration of the vertices of INN-POL. If $PQR$ is a triangle in FIRPOL whose affine hull with expansion coefficients greater than or equal to $-\varepsilon_C$ encloses INNPOL, then each $\mathcal{I}_i$ is an affine combination of $P$, $Q$ and $R$ with

$$\mathcal{I}_i = \alpha_i P + \beta_i Q + \gamma_i R$$

and $\alpha_i + \beta_i + \gamma_i = 1$ together with $\alpha_i, \beta_i, \gamma_i \geq -\varepsilon_C$. These expansion coefficients depend on the index $i$ of the vertex.

In the following we analyze three different cases: Namely we assume that for two of the three vertices $P$, $Q$ and $R$ all expansion coefficients are strictly greater than $-\varepsilon_C$. We derive for each of these three cases a contradiction. This finally proves the theorem.

**Case I:** Suppose that the coefficients of $P$ and $Q$ are strictly greater than $-\varepsilon_C$ for each vertex of INNPOL, i.e. $\alpha_i > -\varepsilon_C$ and $\beta_i > -\varepsilon_C$ for each vertex $\mathcal{I}_i$ of INN-POL. Let $Q'$ be a convex combination of $P$ and $Q$

$$Q' = \lambda P + (1 - \lambda)Q$$

with $0 < \lambda < 1$. The point $Q$ can be expressed as $Q = (Q' - \lambda P)/(1 - \lambda)$. Inserting this in the affine representation of $\mathcal{I}_i$ results in the affine combination of $P$, $Q'$ and $R$

$$\mathcal{I}_i = \underbrace{\left(\alpha_i - \frac{\lambda \beta_i}{1 - \lambda}\right)}_{\bar{\alpha}_i} P + \underbrace{\frac{\beta_i}{1 - \lambda}}_{\bar{\beta}_i} Q' + \gamma_i R.$$

Now it is possible to choose $0 < \lambda_0 < 1$ sufficiently small so that the coefficients $\bar{\alpha}_i = \alpha_i - (\lambda_0 \beta_i)/(1 - \lambda_0)$ and $\bar{\beta}_i = (\beta_i)/(1 - \lambda_0)$ are greater than $-\varepsilon_C$ for all indexes $i$ (as we have assumed $\alpha_i > -\varepsilon_C$ and $\beta_i > -\varepsilon_C$). Then let

the point $Q''$ be the point of intersection of the boundary of FIRPOL with a ray starting in $R$ and passing through $Q'$. The geometry of this construction is illustrated in Figure 12.

Next the point $Q'$ can be expressed as a convex combination of $Q''$ and $R$ in the form

$$Q' = \mu Q'' + (1 - \mu)R$$

with a parameter $0 < \mu < 1$. Then the vertices of INN-POL can be written as

$$\mathcal{I}_i = \bar{\alpha}_i P + \mu \bar{\beta}_i Q + (\gamma_i + (1 - \mu)\bar{\beta}_i)R,$$

see Figure 12. The coefficients $\bar{\alpha}_i$ and $\mu \bar{\beta}_i$ are strictly greater than $-\varepsilon_C$. Suppose $\gamma_i + (1 - \mu)\bar{\beta}_i < -\varepsilon_C$ to be valid, then $\gamma_i$ and $\bar{\beta}_i$ must each be negative, which contradicts the fact that $P$ is located on the boundary of FIRPOL. Since $\gamma_i$ and $\bar{\beta}_i$ cannot both be negative, the equality $\gamma_i + (1 - \mu)\bar{\beta}_i = -\varepsilon_C$ holds, if and only if $\gamma_i = -\varepsilon_C$ and $\bar{\beta}_i = 0$ is valid. This would mean that the point $\mathcal{I}_i$ is located outside FIRPOL, which is again a contradiction. Therefore all expansion coefficients are strictly greater than $-\varepsilon_C$. For this case, Lemma 4.5 says that $R$ cannot be located on the inner boundary of the AFS. This means that the assumption of $\alpha_i > -\varepsilon_C$ and $\beta_i > -\varepsilon_C$ cannot hold for all vertices $\mathcal{I}_i$ of INNPOL.

**Case II:** Now we assume $\alpha_i > -\varepsilon_C$ and $\gamma_i > -\varepsilon_C$ for all vertices $\mathcal{I}_i$. The point $R'$ is defined as a convex combination of $P$ and $R$

$$R' = \lambda P + (1 - \lambda)R$$

with $0 < \lambda < 1$. Then $R$ is given by $R = (R' - \lambda P)/(1 - \lambda)$. Now the vertices of INNPOL $\mathcal{I}_i$ can be expressed as affine combinations of $P$, $Q$ and $R'$

$$\mathcal{I}_i = \left(\alpha_i - \frac{\lambda \gamma_i}{1 - \lambda}\right)P + \beta_i Q + \frac{\gamma_i}{1 - \lambda}R'$$

and it is possible to choose a parameter $0 < \lambda_0 < 1$ sufficiently small so that the expansion coefficients $\alpha_i - (\lambda_0 \gamma_i)/(1 - \lambda_0)$ and $(\gamma_i)/(1 - \lambda_0)$ are greater than or equal to $-\varepsilon_C$ for all vertices of INNPOL, and for at least one coefficient equality holds. But this means that $PQR'$ is a triangle, which is included in the triangle $PQR$ and whose affine hull with expansion coefficients greater than or equal to $-\varepsilon_C$ encloses INNPOL. Then $R$ cannot be a point of the inner boundary of the AFS according to Definition 4.4. Therefore the assumption $\alpha_i > -\varepsilon_C$ and $\gamma_i > -\varepsilon_C$ has led to a contradiction.

**Case III:** The assumption $\beta_i > -\varepsilon_C$ and $\gamma_i > -\varepsilon_C$ for each vertex $\mathcal{I}_i$ of INNPOL results a contradiction by the arguments as used for the case II. This completes the proof. $\square$

13

Assume each vertex of INNPOL to be an affine combination of the points $P$, $Q$ and $R$ with expansion coefficients greater than or equal to $-\varepsilon_C$. Further, for one vertex of INNPOL the expansion coefficient of $P$ is assumed to be equal to $-\varepsilon_C$. Thus each vertex $\mathcal{I}_i$ of INNPOL can be written as

$$\mathcal{I}_i = \alpha_i P + \beta_i Q + \gamma_i R$$

with $\alpha_i + \beta_i + \gamma_i = 1$ and $\alpha_i, \beta_i, \gamma_i \geq -\varepsilon_C$. If $\varepsilon_C P$ is added to the latter equation and the sum is divided by $1 + \varepsilon_C$, then the result is

$$\frac{\mathcal{I}_i + \varepsilon_C P}{1 + \varepsilon_C} = \frac{\alpha_i + \varepsilon_C}{1 + \varepsilon_C} P + \frac{\beta_i}{1 + \varepsilon_C} Q + \frac{\gamma_i}{1 + \varepsilon_C} R. \quad (11)$$

Since the sum of the expansion coefficients on the right-hand side of (11) equals 1, the point $(\mathcal{I}_i + \varepsilon_C P)/(1 + \varepsilon_C)$ is an affine combination of $P$, $Q$ and $R$. If $\alpha_i = -\varepsilon_C$ holds, then $(\mathcal{I}_i + \varepsilon_C P)/(1 + \varepsilon_C)$ is on the line through $Q$ and $R$. Otherwise the point is located on the same side of this line as $P$ because the coefficient $(\alpha_i + \varepsilon_C)/(1 + \varepsilon_C)$ is positive.

In the line-moving algorithm sets of shifted points of INNPOL $\mathcal{I}_P$ and $\mathcal{I}_Q$ are used to construct points within the AFS, see Eqs. (5) and (6). The set $\mathcal{I}_P$ is given by the points $(\mathcal{I}_i + \varepsilon_C P)/(1 + \varepsilon_C)$ we examined above. Equivalent conditions can be formulated for the point $Q$ and the set $\mathcal{I}_Q$. From Theorem 4.6 follows that it is sufficient to search for points on the inner boundary of the AFS on the tangents to the sets $\mathcal{I}_P$ and $\mathcal{I}_Q$. This is exactly what is done in the line-moving algorithm.

**Remark 4.7.** *At the end of this section we would like to comment on the position of the constructed points $R$ in the AFS. On the one hand, the tangent-algorithm in Section 3.1 guarantees that the constructed points $R$ are located on the boundary of the AFS. On the other hand, the line-moving algorithm does not necessarily construct AFS elements $R$ in a way that they belong to the inner boundary of the AFS, cf. Definition 4.4. In order to check whether or not $R$ belongs to the inner boundary, one has to try to decrease a feasible triangle $PQR$ to $PQR'$ with $R'$ moved closer to INNPOL so that $PQR'$ still includes INNPOL. If this is possible, then $R$ does not belong to the inner boundary.*

## 5. Numerical experiments

Next the line-moving algorithm is to be tested for a model problem and with respect to different levels of (pseudo-random) noise. For these investigations our focus is on the effect of the parameters $\varepsilon_C$, $\delta d$ and $\delta \phi$.

The same model problem has already been used in the first part of this paper [7] for a comparison of the line-moving algorithm with the polygon inflation algorithm and the classical Borgen plots. Additionally, we consider an example problem of an AFS with two line-shaped segments which is computed by the tangent-algorithm. If we apply the line-moving algorithm and if we allow small negative entries in the factors $C$ and $A$, then the line-shaped AFS segments grow to thin stripes.

### 5.1. The model problem

The three concentration profiles of our three-component model problem are taken as

$$c_1(t) = \exp(-(t - 20)^2/150),$$
$$c_2(t) = \exp(-(t - 50)^2/200),$$
$$c_3(t) = \exp(-(t - 70)^2/250)$$

with $0 \leq t \leq 100$. The associated pure component spectra are

$$a_1(x) = \exp(-(x - 50)^2/500)$$
$$\qquad + 0.5\exp(-(x - 125)^2/500) + 0.1,$$
$$a_2(x) = \exp(-(x - 100)^2/740)$$
$$\qquad + 0.4\exp(-(x - 100)^2/1500) + 0.15,$$
$$a_3(x) = \exp(-(x - 150)^2/1000)$$
$$\qquad + 0.3\exp(-(x - 75)^2/2500) + 0.2$$

for $0 \leq x \leq 200$. The time and the frequency axes are each discretized to 0.5 units so that the resulting matrix $D_0$ of mixture data has the dimensions $201 \times 401$. Figure 13 shows the concentration profiles and pure component spectra.

Normal distributed noise $\sigma$ with a standard deviation of 0.15 is added to $D_0$ in a way which cuts off any negative entries

$$D(i, j) := \max\left((1 + \sigma)D_0(i, j), 0\right).$$

### 5.2. Effects of the parameter selection on the line-moving algorithm

The AFS of $D$ with respect to FSV-scaling and for the parameters $\varepsilon_C = 0.01$, $\varepsilon_A = 0.005$, $\delta d = 0.0001$ and $\delta \phi = 0.1$deg is plotted in Figure 14.

This AFS is used as a reference in order to compare the accuracy of the AFS approximations for different parameter settings. The control parameters $\delta \phi$ and $\delta d$ are chosen relatively small to guarantee a high resolution or accuracy of the computed AFS. We have used a standard PC with a 2.93GHz Intel CPU and with 8 GB
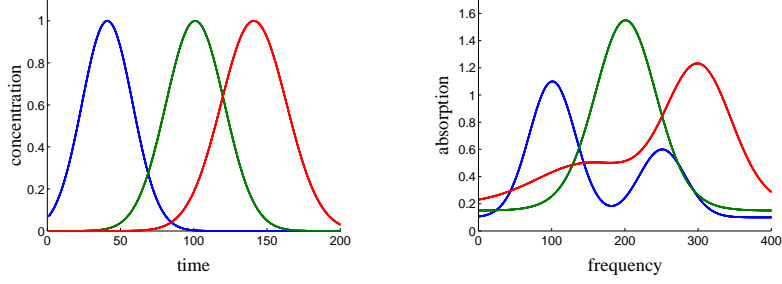
14

Figure 13: The model problem. Left: Concentration profiles. Right: Pure component spectra. (1,2,3)=(Blue, Green, Red).
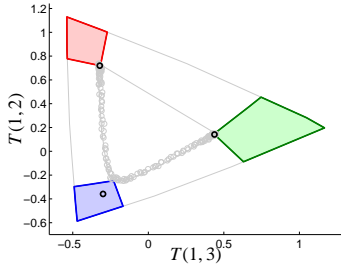


Figure 14: The AFS for the model problem with normal distributed noise (standard deviation $\sigma = 0.15$) computed for the parameters $\varepsilon_C = 0.01$, $\varepsilon_A = 0.005$, $\delta d = 0.0001$ and $\delta\phi = 0.1$ (degrees).

| $\delta\phi$ [deg] | computation time | Hausdorff distance |
|---|---|---|
| 0.1 | 198.9292s | 0 |
| 0.2 | 74.6640s | $2.68 \cdot 10^{-5}$ |
| 0.5 | 30.5176s | 0.0011 |
| 0.7 | 22.1705s | 0.0012 |
| 1 | 15.9477s | 0.002 |

Table 1: Computation times in seconds for the AFS with different values of the parameter $\delta\phi$. The remaining parameters are fixed to $\varepsilon_C = 0.01$, $\varepsilon_A = 0.005$ and $\delta d = 0.0001$. The small Hausdorff distances of the AFS to the reference-AFS (with $\delta\phi = 0.1$ degrees) are tabulated in the right column.

| $\delta d$ | computation time | Hausdorff distance |
|---|---|---|
| $1.0 \cdot 10^{-4}$ | 198.9292s | 0 |
| $5.0 \cdot 10^{-4}$ | 30.0994s | $5.2359 \cdot 10^{-5}$ |
| $1.0 \cdot 10^{-3}$ | 15.3952s | $8.3515 \cdot 10^{-5}$ |
| $5.0 \cdot 10^{-3}$ | 4.0317s | $3.2512 \cdot 10^{-4}$ |
| $1.0 \cdot 10^{-2}$ | 2.5332s | $4.527 \cdot 10^{-4}$ |

Table 2: Computation times in seconds for the AFS computation by the line-moving algorithm with different settings of the parameter $\delta d$. The remaining parameters are fixed to $\varepsilon_C = 0.01$, $\varepsilon_A = 0.005$ and $\delta\phi = 0.1$ (degrees). The column "Hausdorff distance" contains the distances to the reference-AFS with $\delta d = 0.0001$.

RAM for all numerical experiments. The program code is written in C and uses the Matlab graphical user interface (GUI) of the *FACPACK* software. The numerical results are listed in the Tables 1, 2 and 3.

First we study the rotation angle increment $\delta\phi$ by which the tangent is rotated around INNPOL and which is the starting point for the construction of a triangle in FIRPOL which encloses INNPOL. If $\delta\phi$ is halved, then twice as much tangents to INNPOL are used for the AFS construction. Then the computational costs grow approximately by the factor two. This behavior is documented by Table 1. A reasonable balance between the computational costs and accurate AFS approximations is achieved by the default value for $\delta\phi$ which is 0.1 (degrees) in the *FACPACK* software.

Second, the parameter $\delta d$ describes the distance between parallel lines in the line-moving algorithm. Again, halving $\delta d$ approximately doubles the required computing times. In the *FACPACK* toolbox the default value is $\delta d = 0.001$. The results for different settings of $\delta d$ are listed in Table 2.

Finally, we examine the influence of the parameter $\varepsilon_C$ which bounds the smallest entries of $C$ from below, i.e. $C \geq -\varepsilon_C$. For $\varepsilon_C = 0$ the classical tangent al-

15

| $\varepsilon_C$ | computation time | Hausdorff distance |
|---|---|---|
| 0 | 2.5445s | 0.0173 |
| $1.0 \cdot 10^{-4}$ | 181.5765s | 0.0171 |
| $5.0 \cdot 10^{-4}$ | 163.6554s | 0.0183 |
| $1.0 \cdot 10^{-3}$ | 186.6769s | 0.0173 |
| $5.0 \cdot 10^{-3}$ | 162.0274s | 0.0065 |
| $1.0 \cdot 10^{-2}$ | 198.9292s | 0 |
| $5.0 \cdot 10^{-2}$ | 258.6348s | 0.0423 |

Table 3: Computation times in seconds for the AFS with different settings of $\varepsilon_C$. The remaining parameters were fixed to $\varepsilon_A = 0.005$, $\delta\phi = 0.1$ (degrees) and $\delta d = 0.001$. The Hausdorff distances refer to the reference value $\varepsilon_C = 0.01$.
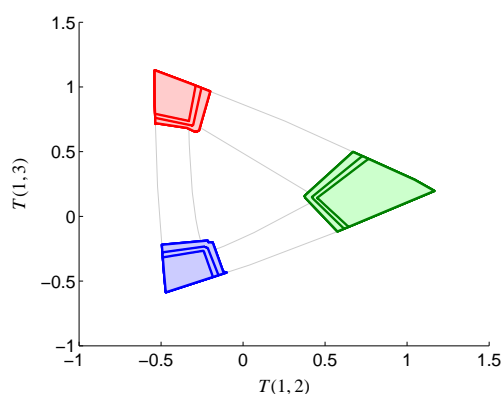


Figure 15: Effect of a growing size (surface area) of the AFS for an increasing value of the parameter $\varepsilon_C$. The parameter $\varepsilon_C$ is set to the four values 0, 0.02 and 0.05. The remaining parameters are fixed to $\varepsilon_A = 0.005$, $\delta\phi = 0.1$ degrees and $\delta d = 0.0001$. The smallest AFS segments of each of the three segments of the AFS belongs to $\varepsilon_C = 0$ and the largest belongs to $\varepsilon_C = 0.05$.

gorithm is used to compute the AFS; only less than 3 seconds are required for this computation. For $\varepsilon_C > 0$ the computation times considerably increase as the line-moving algorithm constructs a larger number of parallel shifted tangents. Interestingly the computation times do not monotonously increase with growing $\varepsilon_C$. However, the largest computation time was found for the largest value of $\varepsilon_C$. The results are given in Table 3.

The parameters $\delta d$ and $\delta\phi$ characterize the spatial resolution of the AFS computation, whereas $\varepsilon_C$ and $\varepsilon_A$ have a direct influence on the size (i.e. the surface area) of the AFS. The parameters $\varepsilon_C$ and $\varepsilon_A$ are to be chosen properly with the knowledge of the smallest acceptable entries of $C$ and $A$ and with the knowledge to which extent the spectral raw data has been perturbed. The effect of $\varepsilon_C$ on the AFS is illustrated in Figure 15.

*5.3. Line-moving algorithm for line-shaped segments*

If a point of INNPOL is located on the boundary of FIRPOL, then the AFS is empty or consists either of a one-point segment or a line-shaped segment. This case occurs if the matrix $D$ has a zero entry (or in the case of perturbed data: an entry equal to $-\varepsilon_A$). If $\varepsilon_A$ is greater than $-\min(D, 0)$, then none of the segments are degenerated, but all segments have a nonzero surface area. Additionally, the case $\varepsilon_A = -\min(D, 0)$ and $\varepsilon_C \geq 0$ does not result in single-point or line-shaped AFS segments. An example is given in Figure 16.

The *FACPACK* module *Generalized Borgen plots* can compute one-point or line-shaped AFS segments if the $\varepsilon$ parameters are set to 0. However, the necessary zero entries of $D$ make this situation numerically less stable compared to the general case.

## 6. Conclusion

The new line-moving algorithm breaks the limitation of the classical tangent algorithm for the construction of Borgen plots. Generalized Borgen plots can be constructed for noisy and perturbed experimental spectral data which can even include slightly negative matrix entries, which can result, e.g., from a background subtraction. We hope that generalized Borgen plots resulting from the line-moving algorithm can be a valuable tool for a deeper understanding of the rotational ambiguity underlying MCR-methods. Generalized Borgen plots combine the strength of a geometric construction of the AFS with various options to control and steer the computations for a proper treatment of perturbed and noisy data.

The line-moving algorithm is implemented in the generalized Borgen plot module of the *FACPACK* software. All results can directly be compared, e.g., with the purely numerical approximation of the AFS by the polygon inflation algorithm.

## References

[1] H. Abdollahi, M. Maeder, and R. Tauler. Calculation and Meaning of Feasible Band Boundaries in Multivariate Curve Resolution of a Two-Component System. *Anal. Chem.*, 81(6):2115–2122, 2009.

[2] O.S. Borgen, N. Davidsen, Z. Mingyang, and Ø. Øyen. The multivariate N-Component resolution problem with minimum assumptions. *Microchimica Acta*, 89:63–73, 1986.

[3] O.S. Borgen and B.R. Kowalski. An extension of the multivariate component-resolution method to three components. *Anal. Chim. Acta*, 174:1–26, 1985.

[4] N. Gillis and F. Glineur. On the geometric interpretation of the nonnegative rank. *Linear Algebra Appl.*, 437(11):2685 – 2712, 2012.
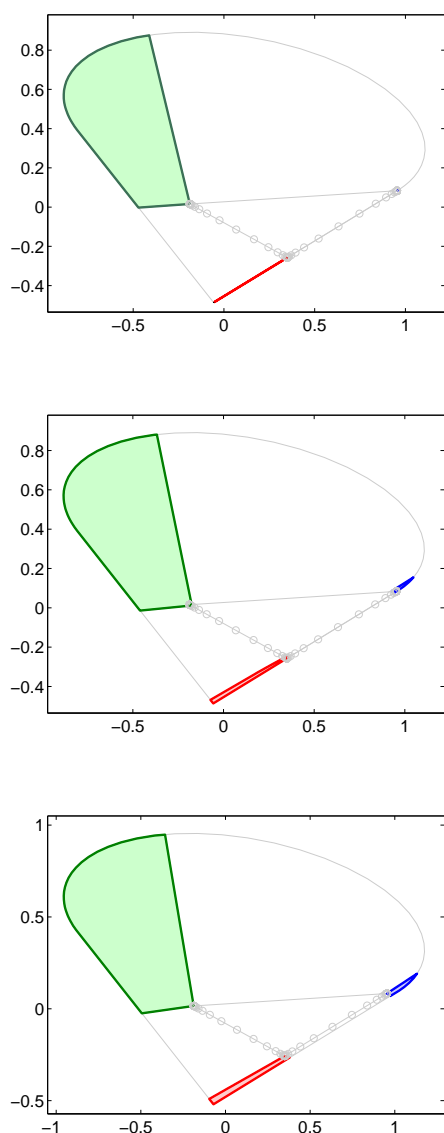
Figure 16: Top: An AFS where one face of INNPOL is located on the boundary of FIRPOL. The AFS for $\varepsilon_C = \varepsilon_A = 0$ is constructed by the classical tangent algorithm of Borgen. The resulting AFS consists of two line-shaped AFS segments and a third AFS segment with a nonzero surface area. Center: The Generalized Borgen plot for the same problem with $\varepsilon_C = 0.01$ and $\varepsilon_A = 1.0 \cdot 10^{-6}$. The line-shaped AFS segments have grown to thin stripes with a nonzero surface area. Bottom: The AFS with $\varepsilon_C = 0$ and $\varepsilon_A = 0.01$.

[5] A. Golshan, M. Maeder, and H. Abdollahi. Determination and visualization of rotational ambiguity in four-component systems. *Anal. Chim. Acta*, 796(0):20–26, 2013.

[6] G.H. Golub and C.F. Van Loan. *Matrix Computations*. Johns Hopkins Studies in the Mathematical Sciences. Johns Hopkins University Press, Baltimore, MD, 2012.

[7] A. Jürß, M. Sawall, and K. Neymeyr. On generalized Borgen plots. I: From convex to affine combinations and applications to spectral data. *J. Chemom.*, 29(7):420–433, 2015.

[8] W.H. Lawton and E.A. Sylvestre. Self modelling curve resolution. *Technometrics*, 13:617–633, 1971.

[9] R. Rajkó. Studies on the adaptability of different Borgen norms applied in self-modeling curve resolution (SMCR) method. *J. Chemom.*, 23(6):265–274, 2009.

[10] R. Rajkó and K. István. Analytical solution for determining feasible regions of self-modeling curve resolution (SMCR) method based on computational geometry. *J. Chemom.*, 19(8):448–463, 2005.

[11] R. Rajkó, H. Abdollahi, S. Beyramysoltan, and N. Omidikia. Definition and detection of data-based uniqueness in evaluating bilinear (two-way) chemical measurements. *Anal. Chim. Acta*, 855:21 – 33, 2015.

[12] M. Sawall, A. Jürß, H. Schröder, and K. Neymeyr. *On the analysis and computation of the area of feasible solutions for two-, three- and four-component systems*, volume in Resolving Spectral Mixtures, Ed. C. Ruckebusch, chapter ..., page ... Elsevier, Cambridge, 2016.

[13] M. Sawall, C. Kubis, D. Selent, A. Börner, and K. Neymeyr. A fast polygon inflation algorithm to compute the area of feasible solutions for three-component systems. I: Concepts and applications. *J. Chemom.*, 27:106–116, 2013.

[14] M. Sawall and K. Neymeyr. *How to compute the Area of Feasible Solutions, A practical study and users' guide to FAC-PACK*, volume in Current Applications of Chemometrics, ed. by M. Khanmohammadi, chapter 6, pages 97–134. Nova Science Publishers, New York, 2014.

[15] M. Vosough, C. Mason, R. Tauler, M. Jalali-Heravi, and M. Maeder. On rotational ambiguity in model-free analyses of multivariate data. *J. Chemom.*, 20(6-7):302–310, 2006.